

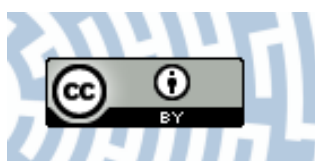


You have downloaded a document from
RE-BUŚ
repository of the University of Silesia in Katowice

Title: Integrated geophysical and geochemical methods applied for recognition of acid waste drainage (AWD) from Zn-Pb post-flotation tailing pile (Olkusz, southern Poland)

Author: Jolanta Pierwoła, Marcin Szuszkiewicz, Jerzy Cabala, Krzysztof Jochymczyk, Bogdan Żogała, Tadeusz Magiera

Citation style: Pierwoła Jolanta, Szuszkiewicz Marcin, Cabala Jerzy, Jochymczyk Krzysztof, Żogała Bogdan, Magiera Tadeusz. (2020). Integrated geophysical and geochemical methods applied for recognition of acid waste drainage (AWD) from Zn-Pb post-flotation tailing pile (Olkusz, southern Poland). "Environmental Science and Pollution Research" 2020 (article in press), doi 10.1007/s11356-020-08195-4



Uznanie autorstwa - Licencja ta pozwala na kopiowanie, zmienianie, rozprowadzanie, przedstawianie i wykonywanie utworu jedynie pod warunkiem oznaczenia autorstwa.



UNIWERSYTET ŚLĄSKI
W KATOWICACH



Biblioteka
Uniwersytetu Śląskiego



Ministerstwo Nauki
i Szkolnictwa Wyższego



Integrated geophysical and geochemical methods applied for recognition of acid waste drainage (AWD) from Zn-Pb post-flotation tailing pile (Olkusz, southern Poland)

Jolanta Pierwola¹ · Marcin Szuskiewicz² · Jerzy Cabala¹ · Krzysztof Jochymczyk¹ · Bogdan Żogała¹ · Tadeusz Magiera²

Received: 17 June 2019 / Accepted: 21 February 2020
© The Author(s) 2020

Abstract

Long-term underground exploitation of Zn-Pb ores has led to drainage of the area and formation of a huge dumping ground in the form of a pile. In its vicinity, processes of acid drainage have developed as a result of contamination of soils and groundwater. Geochemical transformations of mineral contents of waste can significantly affect physical and chemical properties of the soils and the bedrock. At the prospect of termination of the mining activity in the near future, determining the routes of the pollution migration, ability to monitor acid drainage processes and assessment of the risk of heavy metal pollution are really crucial. The paper presents a proposal for solving this problem by means of geophysical methods: Electrical Resistivity Tomography (ERT), Time Domain-Induced Polarisation (TDIP), Frequency Domain Electromagnetics (FDEM) and shallow-depth magnetometric surveys combined with geochemical investigations. The obtained results of geophysical surveys have been confirmed by geochemical investigations. The applied ERT and TDIP methods make it possible to identify the spread of the zones of pollution around the tailing pile, but their effectiveness depends on humidity of the ground. Soil magnetometry and shallow-depth induction profiling are a good tool to identify the medium contaminated with minerals redeposited by aeolian processes and allow to determine the range of the dust spread from the pile. It has been shown that the range of impact of the geochemical changes around the tailing pile is high and depends not only on directions and dynamics of water flow from the pile but also on aeolian transport.

Keywords Acid waste drainage (AWD) · Zn-Pb flotation tailings · Vadoze zone · Geoelectrical and magnetic methods · SEM · EDS · XRD methods

Introduction

Large-scale exploitation and processing of Cu and Zn-Pb ores which has lasted for the last 50 years has led to production of waste, which constitutes about 20% of all industrial waste

deposited in Poland. In the vicinity of Olkusz near Kraków (southern Poland), about 60 million tons of waste from the flotation of Zn-Pb ore of the Mississippi Valley-Type (MVT) has been deposited in the area of ca. 120 ha.

Geochemical transformations of mineral components of the waste, especially in fine-grained fractions, as well as appreciable share of metal-bearing Fe, Zn and Pb sulphides can have a significant impact on the local ecosystem including bedrock, soil, air, groundwater and its biotic elements. The way and scale of this environmental impact is most often assessed on the basis of mineralogical and geochemical analyses (Alpers et al. 1994; Lefebvre et al. 2001; Bucby et al. 2003; Cabala et al. 2004; Bauerek et al. 2009, 2013).

The abovementioned transformations significantly influence the physicochemical properties of soils and the bedrock,

Responsible editor: Philippe Garrigues

✉ Jolanta Pierwola
jolanta.pierwola@us.edu.pl

¹ Faculty of Natural Sciences, University of Silesia, 60 Będzińska St., PL-41-200 Sosnowiec, Poland

² Institute of Environmental Engineering, Polish Academy of Sciences, 34 Skłodowskiej-Curie St., PL-41-819 Zabrze, Poland

thus application of geophysical methods, in particular the geoelectric ones, for understanding the paths of pollution migration seems to be quite promising.

Transfer of the sulphide oxidation products: Zn^{2+} , Cd^{2+} , Pb^{2+} , Mg^{2+} , Ca^{2+} and SO_4^{2-} change the electrical conductivity of the rock mass (Schön 2015). Therefore electrical resistivity and electromagnetic methods are successfully used to identify zones of acid drainage related to exploitation and processing of metal ores (Vanhala et al. 2004; Chouteau et al. 2006; Cabala et al. 2008; Iacob and Orza 2008; Gómez-Ortiz et al., 2010; Nearing et al. 2013; Acosta et al. 2014; Olenchenko et al. 2016; Epov et al. 2017) and of hard coal (Ladwig 1983; Pierwola and Kowalska 2012; Pierwoła 2013; Power et al. 2018).

The induced polarisation method is widely used in environmental studies because it enables to distinguish changes in electrical conductivity due to the presence of mineralised water from those caused by the clayey or conductive minerals.

The range and size of redeposition of the dust fraction from waste dumping grounds, not covered with sod, rich in Fe sulphides can be determined by soil magnetometry methods. The weathering processes cause the iron to pass from the paramagnetic forms to the ferri- or antiferrimagnetic forms, which results in an increase in the value of magnetic susceptibility. The research (Rachwał et al. 2017; Magiera et al. 2018) showed a high correlation between the magnetic susceptibility values and Zn, Mn, Cu, As and Sb, the potentially toxic elements (PTEs) characteristic for emissions associated with storage and processing of Zn-Pb ores.

There have not been any comprehensive geophysical and geochemical investigations in the vicinity of the Olkusz pile with post-flotation tailings after Zn-Pb ore processing, which interpretation would allow to identify the range of pollution and to determine the directions of the pollution transport. The aim of the carried out research has been to assess possibility of application of the set of research methods to identify zones of pollution spreading into the soil and rock mass in the vicinity of the tailing pile. Determination of the extend and dynamics of sulphate ions and heavy metal (HM) transfer is particularly important in case of termination of the exploitation, discontinuation of water mine drainage (WMD) and gradual reconstruction of the original hydrological system, which poses a real threat of pollution to the Triassic part of the karst-fissure drinking water reservoir.

Materials and methods

Area of study

The Zn-Pb ore tailing dumping ground (Fig. 1) was established in the former sand pit at the end of the 1960s. Protection of the substrate against infiltration of leachate from

the dumping ground has been poor due to its location on fluvio-glacial sands, fine and medium grained ones with intercalations of gravel, debris, clay, dust and loam (Motyka et al. 2005). The sands were deposited in the Pleistocene in the paleovalley of the Przemsza River, and their thickness varies from several to about 60 m. Under the sandy sediments, there are carbonate Triassic rocks (Fig. 2). In the area of the dumping ground, they built the tectonic horst Olkusz-Bolesław (Cabala 2001). The Triassic ceiling is of erosive character. On the edges, there are exposures of various Triassic formations: ore-bearing dolomites, Gogolin limestones and Roethian dolomites. The more complete profile of the Triassic formation isolated by impermeable, silty deposits of the Keuper is represented in trough faults, e.g. the Pomorzany graben (Fig. 2).

A complete soil profile has not developed in the vicinity of the dumping ground. In the area of outcrops of carbonate rocks, soils have the characteristics of initial rendzinas or rendzic leptosols or podzols on fluvio-glacial sands (Gruszczynski et al. 1990). In the area of research, there are initial soils (Regosols) and industrial ones (Technosols).

In the hydrogeological system, it is possible to distinguish Quaternary level related to sands, with a filtration coefficient of 2.5×10^{-4} m/s, which has been drained by carbonate, karst-fissure formations of the Triassic level. Fissured and cavernous diplopore and ore-bearing dolomites occurring in the upper Triassic are very well permeable (10^{-5} – 10^{-4} m/s) (Postawa and Motyka 2018). The layers of Olkusz and Gogolin limestones located below contain marl and clay intercalations, hence their permeability is lower—in the order of 10^{-7} – 10^{-5} m/s.

Over 50 years of the underground exploitation of shallow Zn-Pb ore has resulted in drainage of the Quaternary and Triassic levels. The mines, pumping about 200 m³ of water/min, have formed a cone of depression of a diameter of up to 20 km (Motyka et al. 2016; Postawa and Motyka 2018).

Geophysical investigations

Geophysical investigations were carried out along three profiles in close proximity to the tailing dumping ground (Fig. 1). Profile A-B is oriented perpendicularly to the eastern slope of the pile. The C-D profile runs parallel to its northern slope. The third profile P-R, running longitudinally, was delineated on the eastern slope of the pile and served as a reference line.

Along these profiles, the measurements of electrical resistivity (ERT) and induced polarisation (TDIP), with the Lund Imaging System (ABEM); conductometric profilings (FDEM), with conductivity metres EM38-MK2 and EM31-MK2 (Geonics Ltd.); and low-field magnetic susceptibility, using MS2 Bartington susceptibility metre (Bartington Instruments Ltd.) were carried out.

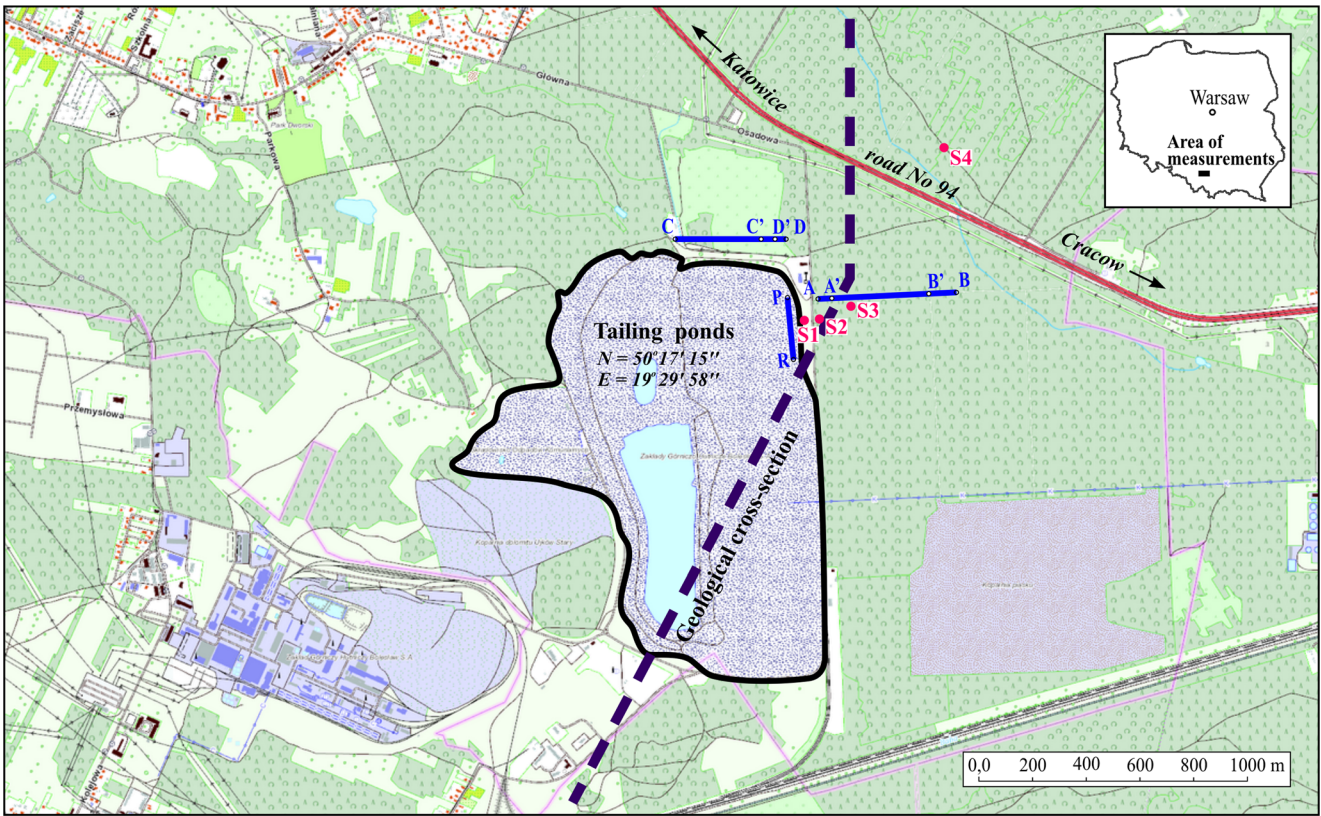


Fig. 1 Location of the investigated area with the lines of geophysical measurements (blue lines) and sampling areas. S1 At a distance of 0 m from tailing pile. S2 50–200 m from tailing pile. S3 300–400 m from tailing pile. S4 1000 m from tailing pile (sampling depth 0–0.8 m)

ERT measurements were conducted using the Wenner-Schlumberger array with the smallest distance between the electrodes $a = 5$ m. The array type and geometry were chosen to

provide suitable depth of recognition, satisfactory resolution and adequate signal level (Loke, 2019) in dry sands of fluvio-glacial origin which was unfavourable for electrical measurements.

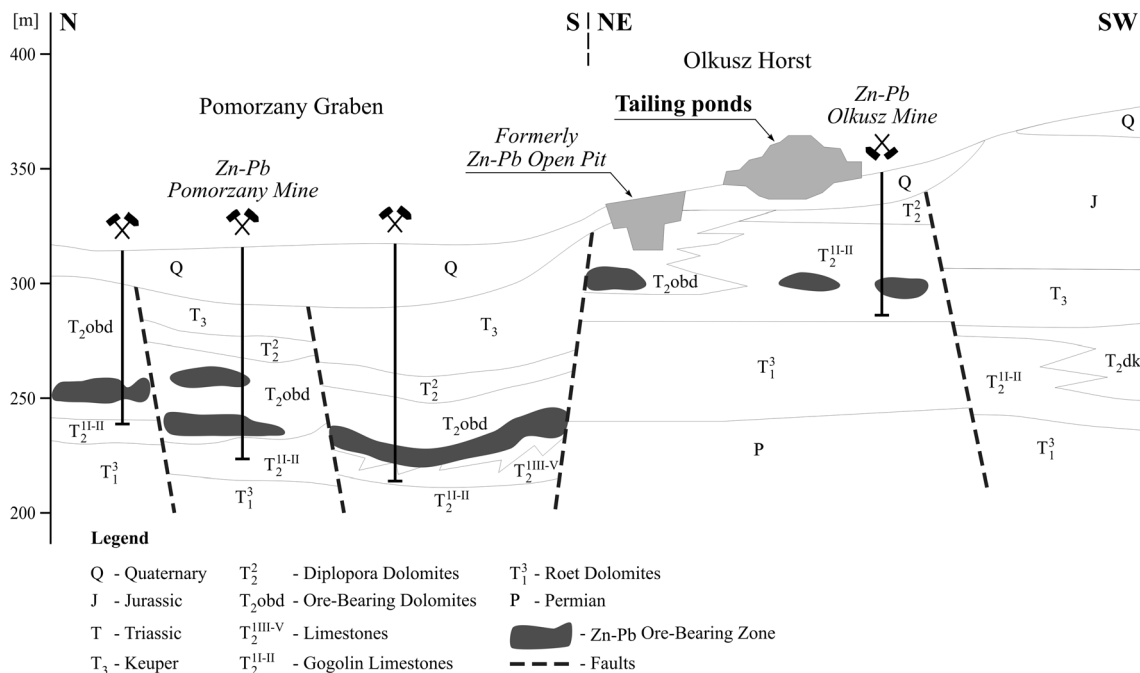


Fig. 2 Geological cross section

Conductometric profilings were made using devices with fixed dipole spacings: 0.5 m, 1.0 m and 3.66 m, which in vertical orientation (VD) enabled recognition to the depths of 0.75 m, 1.5 m and 6 m respectively. The EM surveys have given detailed information from shallow-depth intervals omitted during the ERT. To recognise the anomalous, near-surface intervals of the A-B and C-D lines, identified in EM results, during the induced polarisation measurements, the unit electrode spacing was reduced to $a = 0.5$ m.

For the measurements of volume magnetic susceptibility (κ), which is the ratio of the magnetization to magnetic field (Hunt et al. 1995), the MS2 Bartington metre with MS2D loop probe was used. This probe (with a diameter of 185 mm) has been designed for outdoor use, in particular, for soil surface measurements with a maximum penetration depth of 10 cm; however, 90% of the signal came from the layer not deeper than 6 cm (Dearing 1999; Lecoanet et al. 1999). At each individual location point, geographic coordinates were determined using the GPS system, and 11 MS2D individual readings of soil magnetic susceptibility, evenly distributed within a circle of about 2-m radius, were made. The final κ value was the average of 11 data after statistical evaluation and elimination of outliers.

Collected soil samples (S1–4) for a laboratory magnetic measurements were air dried, homogenised, weighed and placed in plastic container of 10 cm³. Measurements of κ were performed using a MS2 Bartington metre with a MS2B sensor at low (465 Hz) and high (4650 Hz) frequencies. Using the κ value obtained and the sample density, the mass magnetic susceptibility (χ) value was calculated. Additionally, a percentage frequency-dependent magnetic susceptibility ($\chi_{FD\%}$) was computed ($\chi_{FD\%} = (\chi_{465\text{Hz}} - \chi_{4650\text{Hz}}) / \chi_{465\text{Hz}}$) (Dearing, 1999).

Mineralogical analyses

Electron-probe microanalyses and observations were performed using an Environmental Scanning Electron Microscope (Philips XL 30) with an EDS (energy dispersive X-ray spectrometer) analyser. The investigated material (waste, soil and sand) was fixed to carbon tapes (1 × 1.5 cm) placed on aluminium stubs. For each sample, a few hundred representative particles were placed onto the carbon adhesive base and examined using a stereo microscope. Thirty samples of wastes, topsoil and more deeply sandy sediments were viewed uncoated using a SEM with a back-scattered electron (BSE) detector (Centaurus). Eighty qualitative microanalyses (EDS) of minerals of all the 30 samples were carried out using an attached EDS (Sapphire) (15-kV accelerating voltage, environmental mode and 40-Pa H₂O pressure). Ninety BSE images of soil and waste material of all the 30 samples were registered to document the analysed material. The presence of characteristic peaks of some elements in the EDS spectra enabled determination of the elemental compositions.

X-ray diffraction analyses (XRD) of the mineral components were made on soil samples collected on the waste pile (S1) and in its vicinity (S2—50–200 m, S3—300–400 m, S4—1000 m; Fig. 1). They were carried out by means of a Philips PW 3710 X-ray diffractometer (Co $\kappa\alpha$ radiation, 45-kV voltage, 30-mA amperage, impulse counting time 1.2 s, 0.02° step size).

Samples S1, S2, S3 and S4 were subjected also to a high temperature thermomagnetic analysis to determine the major magnetic fractions contributed to the measured magnetic signal. The determination was based on the estimation of the Curie point of dominant magnetic minerals present in the measured material. The analysis were carried out in the temperature range from 20 to 700 °C at a heating rate of 8.5 °C/min using a MFK1 multifunction magnetic susceptibility bridge (AGICO, Brno, Czech Republic), equipped with a CS4 heating chamber. The measurements were conducted both in an air and argon atmosphere.

Results and discussion

Mineralogical data

Tailings, like the Zn-Pb-Fe primary ores, have a carbonate mineral composition (Table 1). Among ore-bearing minerals, there are simple sulphides: sphalerite ZnS, PbS galena, marcasite and FeS₂ pyrite (Kucha and Viaene 1993; Górecka 1996; Viets et al. 1996; Cabala et al., 2004; Sracek et al. 2004). The waste is mainly composed of fine-grained fraction < 0.04 mm (Górecka et al. 1994). They are characterised by high, from 15 to 18%, iron sulphide contents (Cabala et al. 2004; Cabala 2005; Bauerek et al. 2009). XRD analyses proved occurrence of phases which varied concerning their solubility: sulphides, sulphates, carbonates and oxides (Table 1).

Among the wastes which build the slopes of the pile, calcium sulphates (gypsum, rarely basanite) are in abundance. Automorphic crystals which sizes vary from a few to 100 μm were identified on the plant roots epidermis (Fig. 3a). Gypsum has built incrustations on roots (Fig. 3b) and aggregates of aluminosilicates and Fe oxides; it occurs in fine-crystalline grains or submicroscopic accumulations in association with Fe and Zn sulphides (Fig. 3d).

Fe sulphates in the form of isolated grains or submicroscopic crystalline accumulations on aluminosilicate and dolomite aggregates were identified in sediments taken from the depth of 0.2 m (Fig. 3c), as well as 0.6 and 0.8 m.

Sulphate minerals, represented by gypsum, epsomite, copiapite and bianchite, crystallise in large quantity at the places of water discharge on the pile slopes (Fig. 4). The share of the mineral fraction < 0.04 mm, identified as the material from the pile, is over 5% in the soils around the dumping ground. XRD analyses have shown that on the surface of the

Table 1 Mineral composition of the top layer (S1) from tailing ponds (semi-quantitative XRD data)

| | | |
|--|--|--|
| Main gangue components | Dolomite $\text{CaMg}(\text{CO}_3)_2$, ankerite $\text{CaFeMg}(\text{CO}_3)_2$, calcite CaCO_3 , Illite, montmorillonite, kaolinite, quartz SiO_2 | Weak-insoluble Insoluble |
| Sulphides | Marcasite FeS_2 , pyrite FeS_2 , sphalerite ZnS , greenockite CdS , Galena PbS , | Soluble Weak-insoluble |
| Metalliferous carbonates and silicates | Smithsonite ZnCO_3 , cerussite PbCO_3 , Hemimorfite $\text{Zn}_4\text{Si}_2\text{O}_7(\text{OH})_2 \cdot \text{H}_2\text{O}$ | Weak-insoluble Insoluble |
| Sulphates and oxides | Melanterite $\text{FeSO}_4 \cdot 7\text{H}_2\text{O}$, rozenite $\text{FeSO}_4 \cdot 4\text{H}_2\text{O}$, epsomite $\text{MgSO}_4 \cdot 7\text{H}_2\text{O}$, hexahydrate $(\text{Mg,Zn,Fe})\text{SO}_4 \cdot 6\text{H}_2\text{O}$, boyleite $(\text{Zn,Mg})\text{SO}_4 \cdot 4\text{H}_2\text{O}$, bianchite $(\text{Zn,Fe}^{2+})\text{SO}_4 \cdot 6\text{H}_2\text{O}$, copiapite $\text{Fe}_5(\text{SO}_4)_6(\text{OH})_2 \cdot 20\text{H}_2\text{O}$, Gypsum $\text{CaSO}_4 \cdot 2\text{H}_2\text{O}$, bassanite $\text{CaSO}_4 \cdot 0.5\text{H}_2\text{O}$, anglesite PbSO_4 , jarosite $\text{KFe}_3[(\text{OH})_6/(\text{SO}_4)_2]$, Goethite $\text{FeO}(\text{OH})$, Mn oxides, baryte BaSO_4 | Readily soluble Weak-insoluble Insoluble |

pile and in topsoil adjacent to the pile, there is a marked enrichment in Zn-Pb-Fe sulphides, Fe oxides and Zn-Pb carbonates (Table 2). It is important that in sample S1 taken from the initial soil developed on the tailing, the sulphides make up 35% of the mineral composition, with the main sulphides being iron sulphides (marcasite, pyrite). Iron oxides in the waste material constitute only 1%. In soil samples taken outside the pile, the amount of sulphides decreases with the distance. At the same time, the amount of iron oxides increases, reaching 15% in the sample S3 (Table 2). The fine particles containing iron sulphides have been blown out by the wind from the pile and deposited in the soil. Here in oxidising conditions, the sulphides are transformed to iron oxides, which exhibit ferromagnetic properties. This causes the increase of magnetic susceptibility in topsoil in the vicinity of the tailing pile.

This interpretation is confirmed by thermomagnetic analysis. In the case of sample S1 coming from the pile, the analysis performed in an inert environment (argon) has shown the

noticeable increase on the heating curve at approx. 250 °C resulting from the decomposition of sulphides, then a strong peak at about 400 °C where the formation of a ferrimagnetic phase begins (probably a magnetite - Curie point c.a. 580 °C). This phase is unstable and after demagnetization at the Curie temperature retains the characteristics of paramagnetic minerals. During cooling, the sample remains poorly magnetic. At room temperature, the sample has paramagnetic properties and the cooling curve is slightly above the initial κ value of the heating curve (Fig. 5).

The same sample analysed in an oxidising atmosphere behaves differently. The κ value after cooling the sample to room temperature is more than 30 times higher than the initial value, and the sample acquires ferrimagnetic features. The strongly magnetic phase is formed during cooling at a temperature of about 320 °C. This is probably the effect of oxidation of a large amount of sulphides contained in the initial sample, where stable iron oxides form. The same process, although much slower, also occurs in the natural environment in the

Fig. 3 BSE images. **a** Ca sulphates on root epidermis (S2 area). **b** Incrustation of fine-crystalline gypsum on root (S1 area). **c** Fe sulphates in association with FeS i PbS (S3 area) depth 0.2 m. **d** Ca sulphates on Fe sulphates and Pb i Zn sulphides

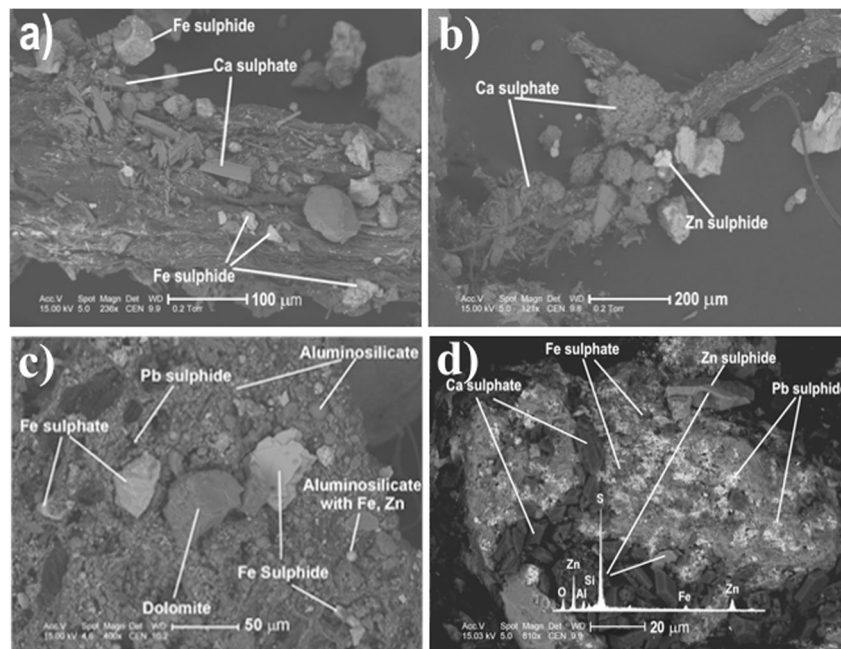




Fig. 4 Sulphate minerals on the slope of the tailing pile

topsoil, where a fine fraction of sulphides entering the soil due to aeolian transport is subject to oxidation processes. As a result, paramagnetic iron sulphides transform into oxide forms with ferrimagnetic properties causing an increase of topsoil magnetic susceptibility in the vicinity of the pile.

Thermomagnetic analyses of soil samples containing lower content of sulphide minerals did not show such a clear effect of sulphide decomposition. In samples S2 and S4, the cooling curve is slightly above the heating curve, and the low initial and final values of the sample indicate relatively small mineralogical changes occurring in the sample during heating. The small amount of oxides present in the sample is probably represented by magnetite. In the case of heating the samples in air, the cooling curve is slightly above the heating curve, but the increase of the κ value after the heating process is relatively small in relation to the initial value.

Table 2 The content of mineral components in the soil from the research area (fraction $\phi < 0.04$ mm, values in % determined on the basis of semi-quantitative XRD analyses)

| Minerals | S1 | S2 | S3 | S4 |
|--------------------------|----|----|----|----|
| Quartz | 6 | 36 | 25 | 52 |
| Dolomite & Fe dolomite | 33 | 25 | 28 | 8 |
| Kalcaite | 10 | 3 | | 5 |
| Markasite | 15 | 10 | 6 | |
| Piryte & sphalerite | 18 | 9 | 8 | 6 |
| Galenite | 2 | | 6 | 1 |
| Cerussite | 8 | | | |
| Smithsonite | 5 | | | |
| Fe oxide & Fe hydroxide | 1 | 2 | 15 | 5 |
| Ca, Zn, Fe, Mg sulphates | 2 | | | 1 |
| K & Na aluminosilicates | | 8 | 3 | 12 |
| Mullite | | 5 | 8 | |
| Kaolinite, illite & mica | | 2 | 1 | 6 |

S1, S2, S3 and S4 areas of sampling in Fig. 1)

A similar pattern is observed in sample S3, showing a higher value of magnetic susceptibility (Table 3). Here, the cooling curve is also above the heating curve and shows a κ value higher in relation to the initial value at room temperature, but the increase in susceptibility in the oxidising environment is not so drastic here (just over 4 times) as compared with sample S1.

Results of geophysical investigations

The longest line of ERT measurement—A-B profile—enabled to carry out geoelectric recognition to the depth of about 70 m. At the depth of about 50 m, in accordance with the geological data from drilling (Central Geological Data Base 2018), the roof of the Middle Triassic dolomite was interpreted. Its resistivity did not exceed 800 Ω m, (Fig. 6). Above it, there was a complex of high-resistivity Quaternary fluvio-glacial sands. In the depth interval of 10–20 m below ground level (bgl), occurrence of sands (probably fine grained) with the resistivity below 2 k Ω m was determined. The subsurface layer built of dry sands, whose thickness was up to 10 m, had the highest resistivity up to 8.5 k Ω m.

The survey was further continued on the lines A-B' and C-D, which were 400 m long each. The measurements were performed twice, i.e. during the long dry period (June–July) when the natural humidity of sand amounted several % (Cabała et al. 2007) and in the period of increased humidity of sediments (March).

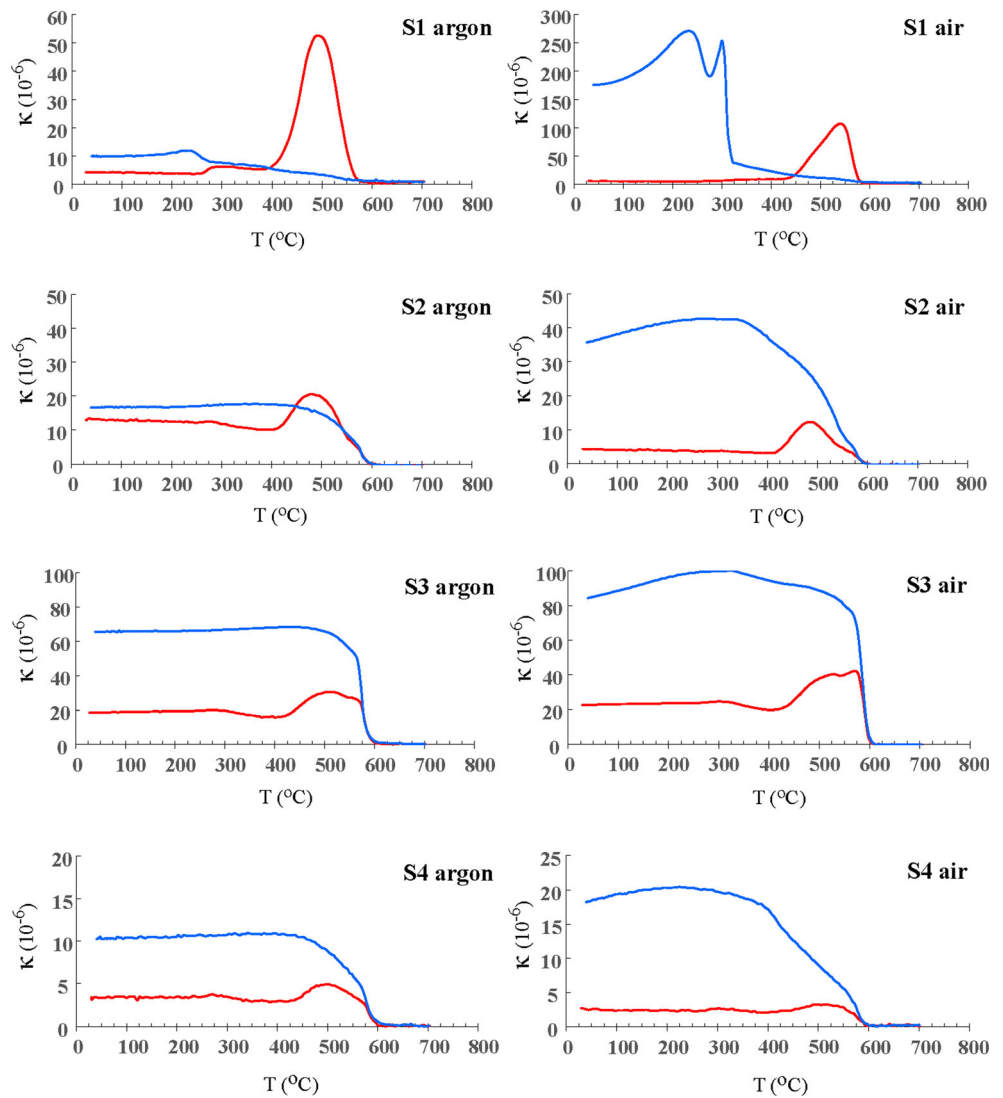
No significant differences in resistivity were observed in both measurement periods in the cross section A-B', surveyed in the interval of 0–20 m bgl. The registered resistivities were high, in the range of 0.8–8 k Ω m (Fig. 7 a and b).

Resistivity survey carried out along the C-D profile showed, in the corresponding depth interval, very strong variation in resistivity depending on the measurement cycle. In dry conditions, the resistivities were identical to those obtained in the A-B' profile (Fig. 8a), while in high humidity conditions, the measured resistivities were significantly lower and did not exceed 200 Ω m (Fig. 8b).

Due to a relatively large initial distance between electrodes ($a = 5$ m), the thin layers closest to the surface might not correspond to the obtained ERT cross sections. Therefore, in order to trace the variability of the electrical conductivity in the most shallow layer, ERT measurements were supplemented by a shallow-depth electromagnetic survey.

In order to determine the conductivity of the tailings, measurements along the 225 m reference profile P-R, on one of the shelves of the eastern slope of the pile, were carried out in the dry period. For both EM-38 depth ranges, up to approximately 180 m of the profile, apparent conductivity values EC_a were stable; around 12–18 mS/m to the depth of 0.75 m and about 8–11 mS/m to the depth of approximately 1.5 m (Fig. 9). The material building the slopes of the pile is homogeneous, hence

Fig. 5 Thermomagnetic curves of samples collected from the waste pile (S1) and from topsoil (S2, S3 and S4), showing changes in magnetic susceptibility with temperature. Measurement conducted in argon and ambient air. Red line, heating curve; blue line, cooling curve



the observed variability may result only from changes in humidity. The average conductivity of dry waste was about 10 mS/m (~100 Ωm). In conditions of high humidity, the conductivity of the waste significantly increased, reaching even 250 mS/m (~4 Ωm) (Pierwoła, 2015). The zone of strong disturbances, visible at the end of the profile at both

depths, correlated with the traces of mass movements on the slope.

Conductometric measurements enabling the survey of distribution of the EC_a of sands in three shallow-depth intervals (0–0.75 m, 0–1.5 m and 0–6 m) were performed, like the resistivity ones, in two cycles (Fig. 10).

The EC_a measured along the A-B' profile in dry conditions was about 5 mS/m lower than the ones obtained in the P-R profile, and its values were approximately 6–7 mS/m in the depth interval of 0–0.75 m, 2–3 mS/m in the interval of 0–1.5 m and 10–11 mS/m in the interval of 0–6 m (Fig. 10a). In all depth intervals, a significant increase of conductivity when compared with the background was observed within the first 20 m of the distance, i.e. in the part closest to the pile. The highest amplitude of the disturbance was observed in the curve of the shallowest profiling, hence it can be assumed that the cause of its occurrence was located just below the ground surface. Measurements repeated during the humid period

Table 3 Average magnetic susceptibility (χ) and percentage frequency-dependent susceptibility (χ_{FD} %) of the tailings and soil samples

| Sample | <i>n</i> | κ ($\times 10^{-5}$ SI units) | χ ($\times 10^{-8}$ m ³ /kg) | χ_{FD} (%) |
|-------------|----------|---------------------------------------|---|-----------------|
| Fresh waste | 10 | 14.0 | 10.0 | 1.2 |
| S1 | 10 | 10.8 | 8.5 | 3.1 |
| S2 | 10 | 33.7 | 25.3 | 4.0 |
| S3 | 10 | 91.5 | 68.5 | 2.2 |
| S4 | 10 | 14.2 | 10.8 | 1.2 |

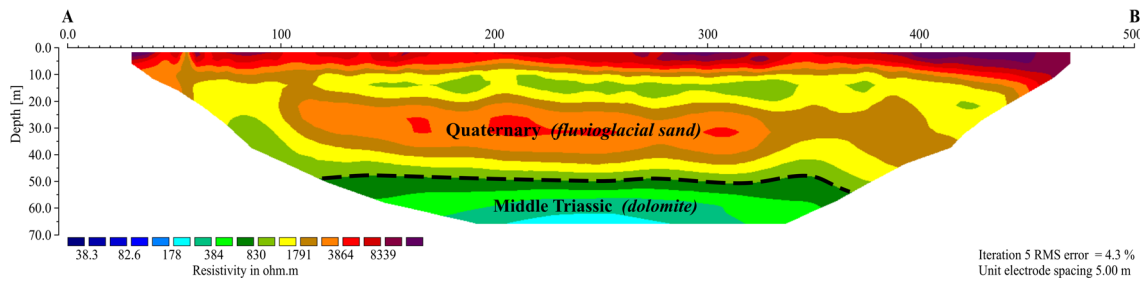


Fig. 6 Deep ERT cross section obtained for the A-B profile

(Fig. 10b) did not show any significant changes in conductivity.

Due to technical reasons, it was necessary to shorten the C-D line by 25 m in relation to the length of the ERT line during the dry period. In that profile, EC_a in the two shallow-depth intervals (Fig. 10c) was significantly higher (5–55 mS/m) in dry conditions comparing with the values obtained in the A-B' profile, and they were close to the values from the P-R lines. The deepest profiling showed EC_a values similar to those obtained on the A-B' line. In two shallow-depth intervals of the C-D profile, the amplitude of conductivity changes reached 60 mS/m; EC_a maxima were observed between 65

and 145 m and 305 and 355 m. The zones of conductivity maxima were recorded in the places of visible traces of landslides on the slopes of the pile. In the parts of the profile located outside the abovementioned anomalous zones, the highest EC_a was recorded within the depth interval of 0–1.5 m.

Contrary to the A-B' line, a rise in EC_a was observed along the C-D profile (Fig. 10d) in the wet period; for two shallow-depth intervals, it varied from a few to approximately 20 mS/m, without any changes of the primary shape of the curves; for the deepest interval (0–6 m), it was 20–30 mS/m, with a significant change of the shape of the obtained curve. Maxima on

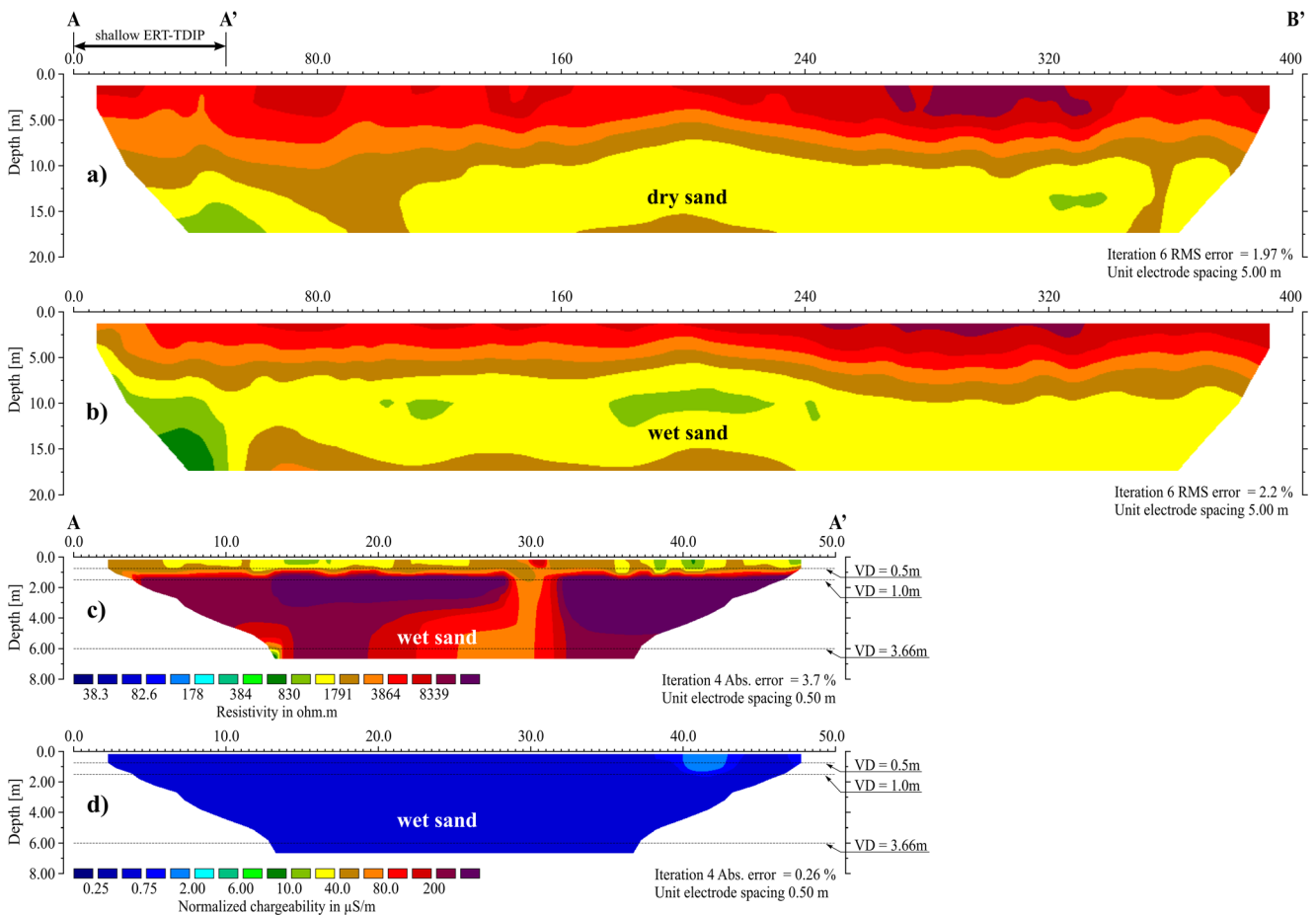


Fig. 7 Geoelectrical cross sections for profile A-B. **a** ERT section for the A-B' interval, dry conditions. **b** ERT section for A-B' interval, wet conditions. **c** Shallow ERT section for A-A' interval, wet conditions. **d** Shallow IP section for the A-A', wet conditions

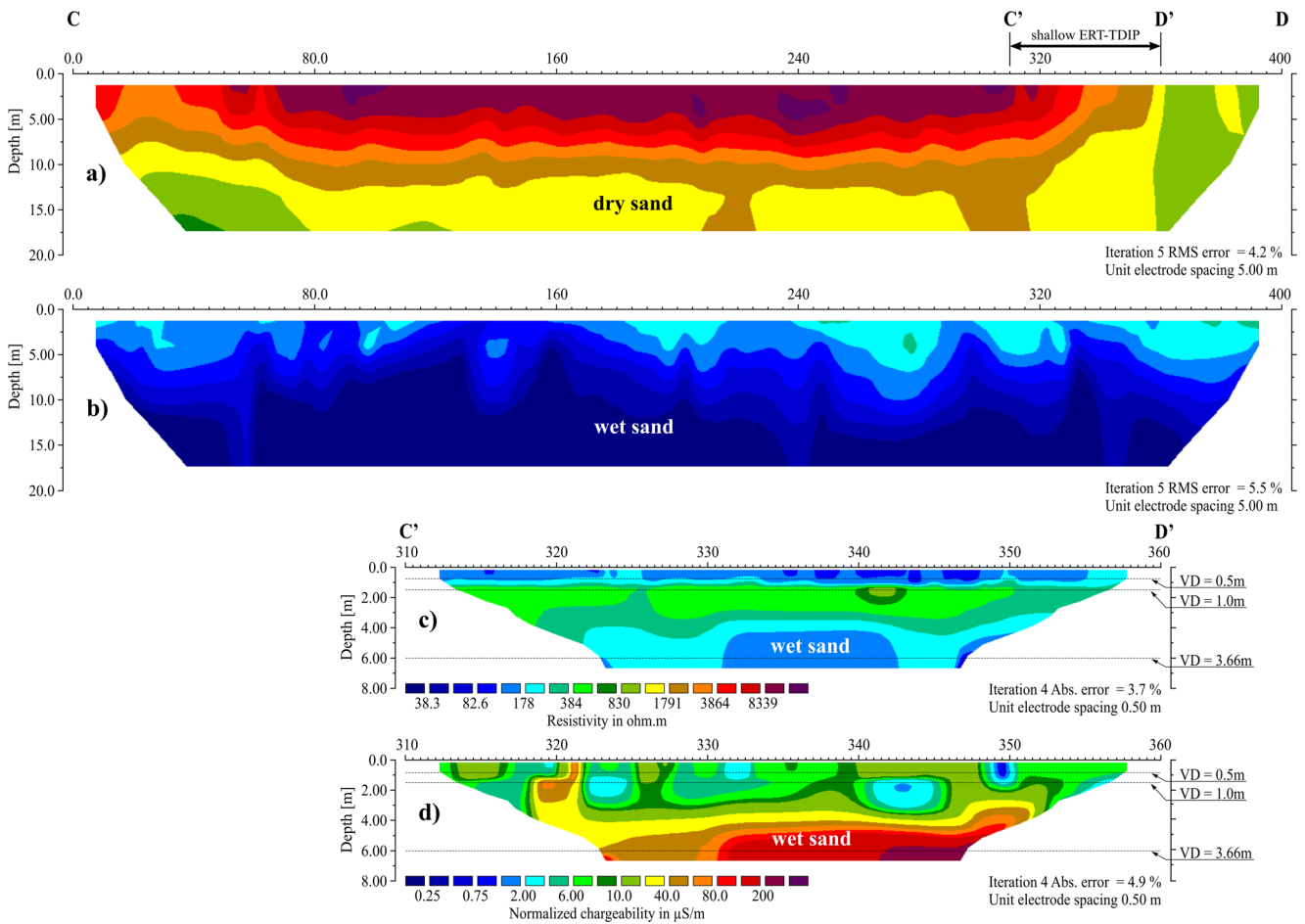


Fig. 8 Geoelectrical cross sections for profile C-D. **a** ERT section for the AC-D interval, dry conditions. **b** ERT section for C-D interval, wet conditions. **c** Shallow ERT section for C'-D' interval, wet conditions. **d** Shallow IP section for the C'-D', wet conditions

the curves obtained from the shallow-depth profiling correlated with the minima on the curve from the deeper profiling.

During the further stage of the investigation, shallow-depth measurements of the induced polarisation were performed in conditions of increased humidity, in the selected zones of the maximum EC_a on both conductometric lines. The line A-A' was determined between 0 and 50 m of A-B' and the C'-D' line between 310 and 360 m of C-D. The depth range was about 6 m, which corresponded to the deepest conductometric survey. The obtained sections, despite the measurement being

performed in stable conditions, differed from each other in the level of observed resistivity (Figs. 7c and 8c) and normalised chargeability (measure of IP effect) (Figs. 7d and 8d). In the section A-A' the resistivity did not drop below 500 Ωm , and the normalised chargeability (MN) was very low (< 0.5–0.75 $\mu S/m$), while along the C'-D' line, the resistivity did not exceed 500 Ωm and the MN was 2–40 $\mu S/m$ to the depth of 3 m, and deeper it increased to approximately 200 $\mu S/m$.

Surface measurement of low-field magnetic susceptibility (κ) of the soil (depth 0.1 m) carried out in the dry

Fig. 9 Apparent conductivity EC_a along the P-R profile situated on the eastern slope of the tailing pile

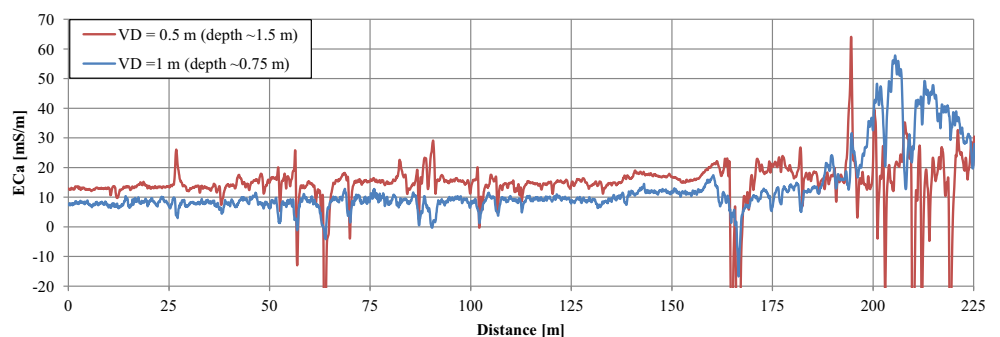
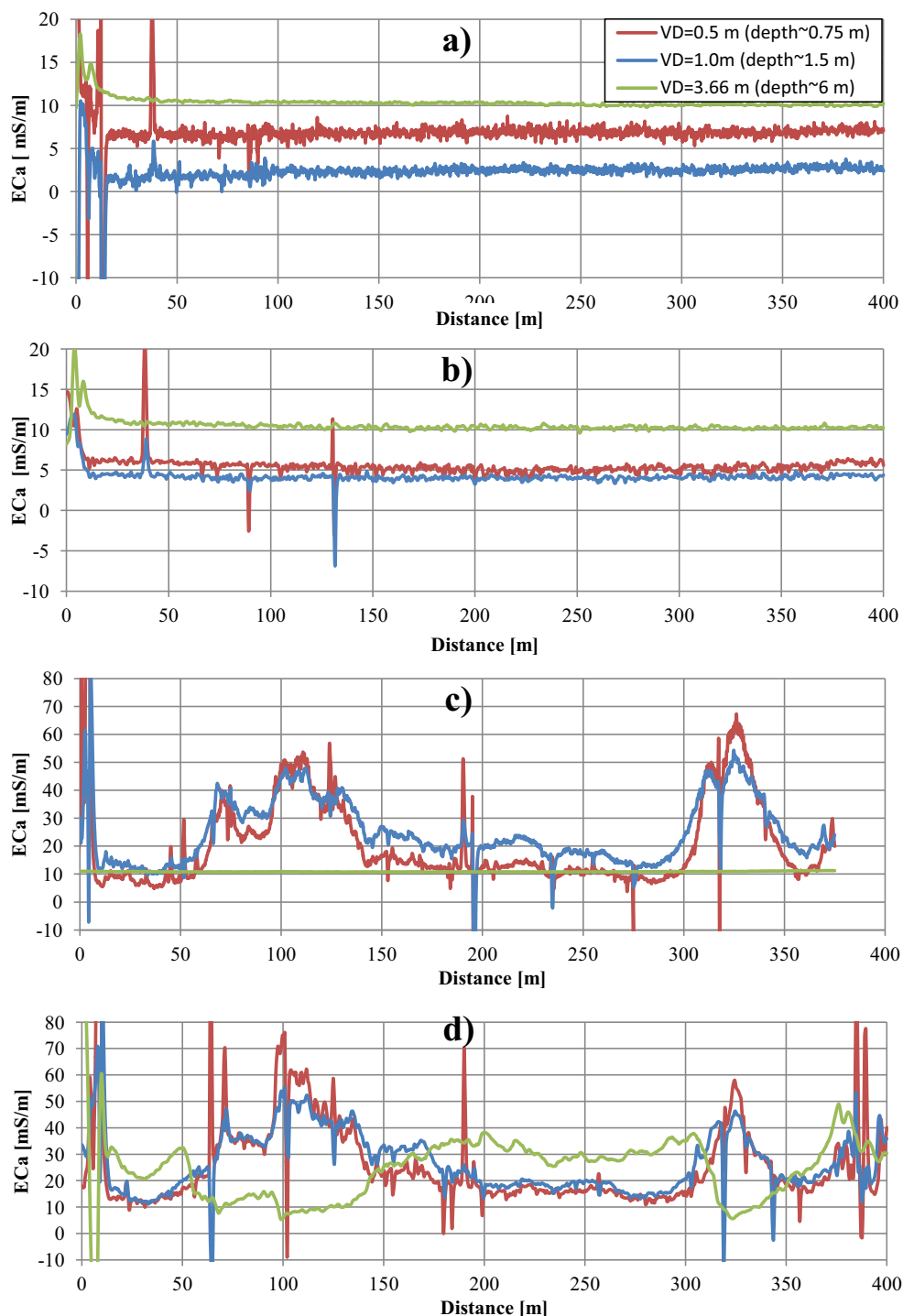


Fig. 10 Apparent conductivity EC_a for search lines. a A-B', dry conditions. b A-B', wet conditions. c C-D, dry conditions. d C-D, wet conditions

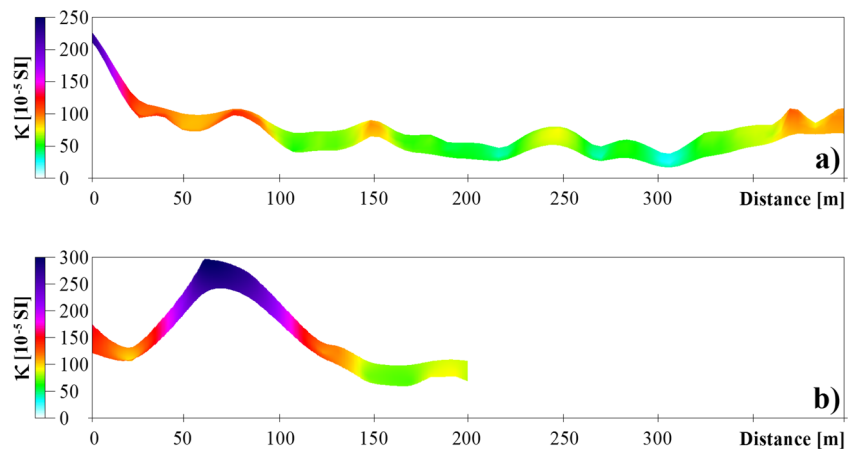


period was the last stage of the survey. The magnetic susceptibility was measured along the profile A-B on the distance of 400 and between 0 and 200 m of the profile C-D. The last 200 m of the profile C-D was not suitable for the surface magnetic measurement due to the local puddles and sawmill waste lying on the surface. Along the A-B profile, measurements were taken in 3 transects at a distance of 10 m from each other. In the

case of C-D profile, measurements were carried out only in 2 transects due to the specific field conditions.

In the A-B profile (Fig. 11a) located in the open ground, east of the pile, the highest magnetic susceptibility values exceeding 200×10^{-5} SI magnetic units occurred in the immediate vicinity of the pile. The value of κ was about 100×10^{-5} SI units over a distance of 25–75 m, while further up to 300 m from the pile, it fluctuated between 30 and 90×10^{-5} SI

Fig. 11 Spatial distribution of mean values of the volume magnetic susceptibility (κ) for A-B (a) and C-D (b) search lines



units. Further than 300 m, the value of κ began to grow again, reaching 100×10^{-5} SI units at a distance of 375–400 m from the pile. The increase has been associated with the morphology of the area (increase of the elevation).

In the western part of the C-D transect (0–40 m), the magnetic susceptibility values remained in the range of $100\text{--}150 \times 10^{-5}$ SI units. In the further part of the profile (along the 40–120-m stretch), there was a rapid increase in the value of κ up to 300×10^{-5} SI units, and then decrease of the values. From 140 m, the κ values remained in the range of $60\text{--}100 \times 10^{-5}$ SI units. A double increase of the κ value (between the 40 and 120 m) corresponded to the fragment of the C-D profile, where a significant increase of relative conductivity on the curves of the shallow-depth electromagnetic profiling was observed (there are visible effects of landsliding processes on the slope of the pile).

Discussion

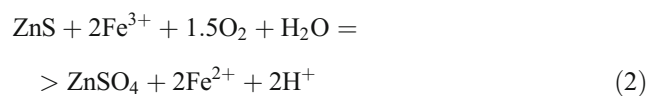
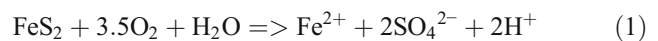
The grounds where tailings of metal ore processing have been dumped impact the environment as a result of various processes: chemical, biological, aeolian, water flow, etc. The purpose of conducting the comprehensive geophysical survey was to test possibilities to detect the most important ones: deep infiltration of mineralised water from the tailing pond through the dumped material, rapid migration of material as a result of surface run-off caused by heavy rains and aeolian transport of the smallest fractions deposited on the pile.

The results of the conducted electrical resistivity and electromagnetic surveys indicate strong response caused by changes of humidity of fluvio-glacial sands adjacent to the tailing pile in the north and the lack of such response in the area located east of the pile. Natural lithological variation of the surveyed material as a possible reason of the observed changes should be excluded.

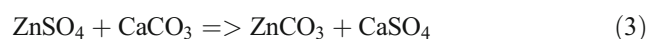
To interpret geophysical surveys properly, it is advisable to identify the area in terms of its mineralogy and geochemistry, which has been confirmed by the results of the earlier works in the areas contaminated by historical wastes from processing of Zn-Pb ore of the MVT type (Cabala et al. 2008).

Carbonate minerals (dolomite and calcite) are the dominating component of the tailings constituting about 73% of the waste, while clay minerals constitute approximately 10%, Zn and Pb carbonates < 1%; the share of Fe sulphides (pyrite and marcasite) (approx. 15–18%) is also significant (Cabala et al. 2004, 2008). Unstable sulphides (FeS₂, ZnS, PbS) and dolomite are the main source of metal ions and sulphates in the migrating waters from the tailings.

Sulphate ions are mobilised, and the Fe²⁺, Zn²⁺ and Mg²⁺ ions are activated in the oxidation reactions of FeS₂ (1) and ZnS (2). The process is less intensive in the case of Pb²⁺.



The Ca²⁺, Mg²⁺, Fe²⁺ and Zn²⁺ ions which are present in the waters enable stabilisation of SO₄²⁻ in hydrous sulphates of Ca (gypsum), Mg (epsomite), Fe (melanterite, copiapite, rozenite) and Zn (bianchite). Fe²⁺ ions are stabilised in Fe oxides and hydroxides (limonites), which form ocher in the shallow layers of the soil. In the carbonate environment of the tailing pile with water deficit, unstable Zn sulphates quickly turn into carbonates (3), and sulphate ions are bound in gypsum.



The processes of leaching and dissolving of sulphides deposited in the tailing pile occur relatively quickly; the process of dissolving hydrated sulphate phases (melanterite, bianchite,

goslarite or gypsum) is even faster. The sulphates, in the form of dispersed crystalline grains were found in large amount in the soils around the pile. During the periods of increased humidity, some of the SO_4^{2-} and heavy metal ions infiltrate into the permeable sandy sediments together with the surface run-off waters. The ions Zn^{2+} , Pb^{2+} , Cd^{2+} , Tl^+ and As^{3+} and also SO_4^{2-} have been released into solutions from metal-bearing minerals, and soils have been contaminated with them (Jambor et al. 2000). Organic matter of the soil causes additional release of OH^- ions, humic, fulvic acids and others.

Despite the fact that the carbonate type of the wastes and bedrock limits the migration of acid solutions, the presence of Fe, Zn and Pb sulphides higher than 15% makes the development of AWD still possible (Cabała 2005).

High buffering properties of post-flotation wastes considerably reduce leaching of SO_4^{2-} , Zn^{2+} , Ca^{2+} , Mg^{2+} and Fe^{2+} ions (Postawa and Motyka 2018), but their quantity transferred from the dump remains high. Motyka et al. (2005) showed that about 5.0 m^3 of leachate containing, on average, 1400 mg/dm^3 of sulphates infiltrates per minute from the tailing ponds to the underlying sediments. The average sulphate content in the water drained by the Pomorzany mine is up to 300 mg/dm^3 (Rózkowski et al. 1997). About 1.42 mg/dm^3 of zinc; up to 0.32 mg/dm^3 of lead; and significant amounts of cadmium, copper, arsenic and nickel are transferred per minute from the pile to the ground (Motyka et al. 2005).

The favourable conditions for the development of acid waste drainage occur in the presence of increased humidity in the investigated area. Significant changes in resistivity/conductivity depending on atmospheric conditions should be interpreted as the result of the occurrence of easily soluble sulphates beyond the tailing pile. The most important reason for the transfer of sulphates is probably inclination of the slopes of the pile, which, with an average precipitation of about 600 mm/year , enable rapid gravitational outflow of rain-water outside the pile boundary.

Laboratory tests of tailings (Cabała et al. 2007) show that the relation of conductivity and humidity is an exponential function, which indicates high levels of easily soluble minerals. Surface run-off water is characterised by mineralisation $300\text{--}600 \text{ mg/dm}^3$, which is mainly caused by sulphates (about 400 mg/dm^3) (Bauerek et al. 2009). It results in high electrical conductivity of the running off water, amounting to an average of $525.4 \text{ }\mu\text{S/cm}$ ($\cong 19 \text{ }\Omega\text{m}$). The water penetrating into the sandy sediments carries acidic products of the drainage, which in the vadoze zone of fluvioglacial sands cannot be buffered in the form of poorly soluble carbonate minerals. As a consequence, hydrous Fe, Mg, Zn and Ca sulphates crystallise. In the periods of increased humidity, sulphates are dissolved in pore spaces, forming electrolytes, which has been reflected in the results of ERT and EM surveys.

The routes of hydraulic transport on the surface of the pile slopes are clearly marked by occurrence of white and yellowish accumulations of sulphate minerals (Fig. 4). The zones of peaks of apparent conductivity (C-D) in shallow conductometric profiles correlate with occurrence of the material sliding down the slopes of the pile. Hence the reduced resistivity, comparing with the A-A' cross section and increased chargeability as well as increased magnetic susceptibility κ (Fig. 11b) associated with secondary iron oxide minerals (Cabała 2005; Table 2) can be interpreted as a result of penetration of fine-grained fractions of the waste material into the layer of fluvioglacial sands at the foot of the pile.

One of the ecological problems of newly formed or old, but poorly turfed tailing piles, is the dusting process. Taking into account the fact that tailings are composed mainly of fine grains $<0.04 \text{ mm}$, the phenomenon can be very intense. Blowing away of fine waste fractions containing various sulphides has led to the spread of the latter in soils in the areas adjacent to the pile. The processes of chemical transformation of Fe sulphides have led to formation of new ferri- or antiferromagnetic phases such as maghemite and haematite. A fine fraction of secondary iron oxides has been removed together with other mineral particles from the unturfed fragments of the pile, and it has been transported by air, resulting in increased magnetic susceptibility of the soils around the pile. Considering low magnetic susceptibility of material (referred to local background) and soils developed on it (with dia- or paramagnetic properties; Łukasik et al. 2016), the increase of magnetic susceptibility in topsoil is due to the deposition of dust containing secondary iron oxides from dusting source (Szuszkiewicz et al. 2016; Jordanova 2016). Hence, the magnetic susceptibility in topsoil is decreasing with the distance from this source. Morphology of the area influences the measured value of κ of the surface layer of soil, causing increased value of κ on local elevations or slopes inclined towards the source of pollution (Fig. 11a). A similar effect was also observed in the area of the post-industrial waste dumping ground of zinc and lead smelter in Piekary (Rachwał et al. 2017).

Aeolian transport may also be the cause of increased apparent conductivity of the most shallow ($\text{VD}=0.5 \text{ m}$) soil layer. Tests of the soil samples taken at the sampling points S1, S2 and S3 (Fig. 1) arranged in accordance with the wind direction dominating in the test area have shown more or less constant content of minerals transported by wind from the pile up to the distance of about 500 m from it. The share of metalliferous minerals decreases with the increase in depth and distance from the pile; however, their occurrence in the topsoil indicates an important role of wind in the

redeposition of grains and mineral aggregates in the zone up to approximately 1.5 km from the tailing pile (S4).

Conclusions

Integrated geophysical and geochemical methods applied in this study enabled identification of different threats related to underground water infiltration, acid waste drainage and dusting processes. Correct identification of zones contaminated with unstable metalliferous minerals should be carried out using the complex of methods: FDEM, ERT, TDIP and soil magnetometry. The results obtained on the basis of the combined geophysical, mineralogical and geochemical methods have shown the range of the impact of ecological changes around the tailing pile. The changes in the chemical properties of the soils around the tailing pile depend not only on the directions and dynamics of the water flow from the pile but also on the aeolian transport responsible for the redeposition of substantial quantities of fine-grained fractions of waste enriched with unstable sulphides, and what more, it was able to identify zones of pollution spreading around the tailing pile.

The geochemical and mineralogical studies revealed the presence of easily soluble, secondary, sulphate mineral phases in the deposited wastes and in their vicinity, which indicates that their crystallisation had been derived from solutions originated in AWD processes. The crystalline sulphate phases Ca, Fe, Mg and Zn occurring in the soils and the sands around the tailing pile are mineralogical markers of the migration routes of the pollutants. Occurrence of unstable, metal-bearing phases is the evidence of the migration of ephemeral electrolyte-type solutions that have a significant impact on the geoelectric and magnetic properties of the rock medium.

The following procedures of geophysical methods have been proposed:

- Induction profiling as a quick and inexpensive method in the initial stage of the study to design the scheme of the further measurements and location of geophysical profiles.
- Soil magnetometry and shallow-depth induction profiling for identifying a zone contaminated with minerals redeposited by aeolian processes and assessing the dusting range of the pile.
- Electrical resistivity methods to assess the range of the zones changed by AWD products and directions of migration pollutants. As this method is strongly dependent on humidity of the sediments, it would be recommended to run the test in at least two cycles (humid and dry periods).

Acknowledgements The authors thank also the professional Proof-Reading-Services.com for language corrections.

Funding information The study was funded by the Polish National Science Centre in the frame of scientific project: no. 2015/17/B/ST10/03335.

Open Access This article is licensed under a Creative Commons Attribution 4.0 International License, which permits use, sharing, adaptation, distribution and reproduction in any medium or format, as long as you give appropriate credit to the original author(s) and the source, provide a link to the Creative Commons licence, and indicate if changes were made. The images or other third party material in this article are included in the article's Creative Commons licence, unless indicated otherwise in a credit line to the material. If material is not included in the article's Creative Commons licence and your intended use is not permitted by statutory regulation or exceeds the permitted use, you will need to obtain permission directly from the copyright holder. To view a copy of this licence, visit <http://creativecommons.org/licenses/by/4.0/>.

References

- Alpers CN, Blowes DW, Nordstrom DK, Jambor JL (1994) Secondary minerals and acid mine-water chemistry. In: Blowes DW, Jambor JL (eds) *The Environmental Geochemistry of Sulfide Mine-wastes*, vol 22. Mineral. Assoc. Canada Short Course Notes, pp 249–269
- Acosta JA, Martínez-Pagan P, Martínez-Martínez S, Faz A, Zornoza R, Carmona DM (2014) Assessment of environmental risk of reclaimed mining ponds using geophysics and geochemical techniques. *J Geochem Explor* 147:80–90
- Bauerek A, Bebek M, Sracek O, Śmieja-Król B (2013) Chemical composition of surface runoff from flotation wastes of Zn–Pb ore formation of the Mississippi Valley-type, Olkusz, southern Poland. *J Geochem Explor* 132:54–62
- Bauerek A, Cabala J, Śmieja-Król B (2009) Mineralogical alterations of Zn–Pb flotation wastes of the Mississippi Valley type ores (southern Poland) and their impact on contamination of rain water runoff. *Pol J Environ Stud* 18(5):781–788
- Bucby T, Black S, Coleman M, Hodson M (2003) Fe-sulphate evaporative mineral precipitates from the Rio Tinto, southwest Spain. *Mineral Mag* 67(2):263–278
- Cabala J (2001) Development of oxidation in Zn-Pb deposits in Olkusz area. In: *Mineral Deposits at the beginning of the 21st century*, Balkema, pp. 121–124
- Cabala J, Teper E, Teper L, Małkowski E, Rostański A (2004) Mineral composition in rhizosphere of plants grown in the vicinity of a Zn-Pb ore flotation tailings pond. Preliminary Study. *Acta Biologica Cracoviensia s Botanica*, 46:65–74
- Cabala J, Idziak A, Kondracka M, Kleczka M (2007) Physical and chemical properties of wastes occurring in areas of historical Zn-Pb ore processing. In: *I konferencja naukowo-techniczna Geologia i geofizyka w rozwiązywaniu problemów współczesnego górnictwa i terenów pogórnicych* (in Polish)
- Cabala J, Żogała B, Dubiel R (2008) Geochemical and geophysical study of historical Zn-Pb ore processing waste dump areas (southern Poland). *Pol J Environ Stud* 17(5):693–700
- Cabala J, (2005) Acid drainage of postflotation wastes from Zn-Pb ores; changes of mineral composition in rhizosphere zones developed on tailings pond. *Zeszyty Naukowe Politechniki Śląskiej, s. Górnictwo*, 267: 63–70 (in Polish)
- Central Geological Data Base. <http://bazagis.pgi.gov.pl/website/cbdg/viewer.htm>. Accessed 19.03.2018

- Chouteau M, Anterrieu O, Aubertin M, Dubreuil-Boisclair C, Poisson J (2006) Geophysical characterization of an AMD-generating waste rock pile using ground and borehole techniques. In: 19th EEGS Symposium on the Application of Geophysics to Engineering and Environmental Problems
- Dearing J. (1999) Environmental magnetic susceptibility. Second edition. http://www.gmw.com/magnetic_properties/pdf/Om0409%20J_Dearing_Handbook_iss7.pdf Accessed 14 March 2019
- Epov M, Yurkevich N, Bortnikova S, Yu K, Saeva O (2017) Analysis of mine waste by geochemical and geophysical methods (a case study of the mine tailing dump of the Salair ore-processing plant). *Russ Geol Geophys* 58:1543–1552
- Gómez-Ortiz D, Martín-Velázquez S, Martín-Crespo T, De Ignacio-San JC, Lillo J (2010) Application of electrical resistivity tomography to the environmental characterization of abandoned massive sulphide mine ponds (Iberian Pyrite Belt, SW Spain). *Near Surf Geophys* 8: 65–74
- Górecka E, Bellok A, Socha J, Wnuk R, Kibitlewski S (1994) Differentiation of metal content in the flotation tailings of Zn-Pb ores (ZGH Bolesław, Olkusz region, SW Poland). *Przeł Geol* 10: 834–841 (in Polish)
- Górecka E (1996) Mineral sequence development in the Zn-Pb deposits of the Silesian-Cracow area, Poland. *Przeł Geol* 154:25–36
- Gruszczyński S, Trafas M, Żuławski CZ (1990) Characteristics of soils in the Olkusz region. *Zeszyty Naukowe AGH Sozologia i Sozotechnika* 32:113–122 (in Polish)
- Hunt CP, Moskowitz BM, Banerjee SK (1995) Magnetic properties of rocks and minerals, in rock physics and phase relations. In: Ahrens TJ (ed) *A handbook of physical constants*. AGU, Washington, pp 189–204
- Iacob C, Orza R (2008) Integrated interpretation of geophysical data on metalliferous mining waste deposits. In: Proc. Near Surface, 14th European Meeting of Environmental and Engineering Geophysics, Kraków, B02
- Jambor JL, Nordstrom DK, Alpers CN (2000) Metal-sulfate salts from sulfide mineral oxidation. In: Alpers CN, Jambor JL, Nordstrom DK (eds) *Sulfate minerals: crystallography, geochemistry, and environmental significance*, *Reviews in Mineralogy and Geochemistry*, vol 40, pp 305–350
- Jordanova N (2016) Soil magnetism: applications in Pedology. In: *Environmental Science and Agriculture*. Academic Press, Elsevier
- Kucha H, Viaene W (1993) Compounds with mixed and intermediate sulfur valences as precursor of banded sulfides in carbonate-hosted Zn-Pb deposits in Belgium and Poland. *Mineral Deposita* 28:13–21
- Ladwig KJ (1983) Electromagnetic induction methods for monitoring acid mine drainage. *Ground Water Monit Remed* 3(1):46–51
- Lecoanet H, Leveque F, Seguna S (1999) Magnetic susceptibility in environmental applications: comparison of field probes. *Phys Earth Planet Inter* 115:191–204
- Lefebvre R, Hockley D, Smolensky J, Gelinac P (2001) Multiphase transfer processes in waste rock piles producing acid mine drainage. Conceptual model and system characterization *J Contam Hydrol* 52:137–164
- Loke MH (2019) Tutorial: 2D and 3D electrical imaging surveys. www.geotomosoft.com. Accessed 14.11.2019
- Łukasik A, Magiera T, Lasota J, Błońska E (2016) Background value of magnetic susceptibility in forest topsoil: assessment on the basis of studies conducted in forest preserves of Poland. *Geoderma* 264: 140–149
- Magiera T, Zawadzki J, Szuszkiewicz M, Fabijańczyk P, Steinnes E, Fabian K, Miszczyk E (2018) Impact of an iron mine and a nickel smelter at the Norwegian/Russian border close to the Barents Sea on surface soil magnetic susceptibility and content of potentially toxic elements. *Chemosphere* 195:48–62
- Motyka J, Adamczyk Z, Czop M, D’Obryn K (2005) Groundwater quality impact by municipal sanitary landfill in Ujków near Olkusz (S Poland). *Gospod Surowcami Min* 21(1):131–153 (in Polish)
- Motyka J, Adamczyk Z, Juško K (2016) The historical view of the water inflows to the Olkusz zinc and lead mines. *Przegląd Górniczy* 6:49–58 (in Polish)
- Nearing G, Tuller M, Jones S, Heinse R, Meding M (2013) Electromagnetic induction for mapping textural contrasts of mine tailing deposits. *J Appl Geophys* 89:11–20
- Olenchenko V, Kucher D, Bortnikova S, Gas’kova O, Edelev A, Gora M (2016) Vertical and lateral spreading of highly mineralized acid drainage solutions (Ur dump, Salair): electrical resistivity tomography and hydrogeochemical data. *Russ Geol Geophys* 57:617–628
- Pierwola J (2013) Investigation of soil contamination using resistivity and induced polarization methods. *Pol J Environ Stud* 22(6):1781–1788
- Pierwola J (2015) Using geoelectrical imaging to recognize Zn-Pb post-mining waste deposits. *Pol J Environ Stud* 24(5):2127–2137
- Pierwola J, Kowalska A (2012) Geoelectrical study of the postmining area in Rudoltowice (Poland). *Remote Sens Environ* 19(1):60–69 ISSN1803-1447
- Postawa A, Motyka J (2018) Selected trace elements in groundwater within Permian sediments near Olusz (Zn-Pb ore mining region, S Poland). *Environ Sci Pollut Res Int* 26(1):34–43
- Power C, Tsourlos P, Ramasamy M, Nivorlis A, Mkandawire M (2018) Combined DC resistivity and induced polarization (TD-IP) for mapping the internal composition of a mine waste rock pile in Nova Scotia, Canada. *J Appl Geophys* 150:40–51
- Rachwał M, Wawer M, Magiera T, Steinnes E (2017) Integration of soil magnetometry and geochemistry for assessment of human health risk from metallurgical slag dumps. *Environ Sci Pollut Res* 24: 26410–26423
- Rózkowski A, Chmura A, Siemiński A (eds) (1997) *Usable ground waters in the upper Silesian Coal Basin and its margin*. Publications of the Polish Geological Institute, CLIX, Warszawa (in Polish)
- Schön JH (2015) Physical properties of rocks. In: *Developments in petroleum science*, vol 65, 2nd edn. Elsevier, Amsterdam
- Sracek O, Choquette M, Gelinac P, Lefebvre R, Nicholson RV (2004) Geochemical characterization of acid mine drainage from a waste rock pile, Mine Doyon, Quebec, Canada. *J Contam Hydrol* 69:45–71
- Szuszkiewicz M, Łukasik A, Magiera T, Mendakiewicz M (2016) Combination of geo- pedo- and technogenic magnetic and geochemical signals in soil profiles—diversification and its interpretation: a new approach. *Environ Pollut* 214:464–477
- Viets JG, Leach DL, Lichte FE, Hopkins RT, Gent CA, Powell JW (1996) Paragenetic and minor- and trace-element studies of Mississippi Valley-type ore deposits of the Silesian-Cracow district, Poland. Publications of the Polish Geological Institute 154:51–71
- Vanhala H, Räsänen M-L, Huotari T, Valjus T, Lehtimäki J, Suppala I (2004) Characterizing tailings impoundment at the closed Hammaslahti Cu-Zn mine, Finland. Proc. Near Surface 2004 - 10th European Meeting of Environmental and Engineering Geophysics, Utrecht, The Netherlands, Z-99

Publisher's note Springer Nature remains neutral with regard to jurisdictional claims in published maps and institutional affiliations.